ORNL/TM-2023/3116

STATUS REPORT OF JOINT RPI/ORNL NCSP TASK FOR THERMAL NEUTRON TOTAL CROSS SECTION MEASUREMENTS

Chris W. Chapman
Kemal Ramic
Jesse Brown
Goran Arbanas

November 2023

OAK RIDGE National Laboratory

ORNL IS MANAGED BY UT-BATTELLE LLC FOR THE US DEPARTMENT OF ENERGY

ORNL/TM-2023/3116

Nuclear Energy and Fuel Cycle Division

STATUS REPORT OF JOINT RPI/ORNL NCSP TASK FOR THERMAL NEUTRON TOTAL CROSS SECTION MEASUREMENTS

Chris W. Chapman
Kemal Ramic
Jesse Brown
Goran Arbanas

November 2023

Prepared by
OAK RIDGE NATIONAL LABORATORY
Oak Ridge, TN 37831
managed by
UT-Battelle LLC
for the
US DEPARTMENT OF ENERGY
under contract DE-AC05-00OR22725

CONTENTS

LIST OF FIGURES

LIST OF TABLES

ABBREVIATIONS

DFPT	density functional perturbation theory
IFC	interatomic force constant
INS	inelastic neutron scattering
LAMMPS	Large-scale Atomic/Molecular Massively Parallel Simulator
LINAC	linear accelerator
MD	molecular dynamics
ORNL	Oak Ridge National Laboratory
PDOS	phonon density of states
PMMA	poly(methyl methacrylate)
RPI	Rensselaer Polytechnic Institute
SNS	Spallation Neutron Source
TCR	Transformational Challenge Reactor
TDEP	temperature-dependent effective potential
TSL	thermal scattering law
VASP	Vienna Ab initio Simulation Package

ABSTRACT

A new cold neutron moderator system was developed and constructed at the Rensselaer Polytechnic Institute (RPI) Gaerttner Linear Accelerator. This system was then used to measure the neutron total cross section in the thermal energy range for polyethylene, polystyrene, Lucite, and yttrium hydride. In tandem with these measurements, a fitting procedure was developed at Oak Ridge National Laboratory to vary computationally simulated phonon density of states until a fit with differential and integral data was achieved. This model, combined with the new RPI total cross section data, was used to generate thermal scattering law files for the materials measured at RPI.

1. INTRODUCTION

Recent efforts have been made to measure double-differential thermal scattering cross sections at the Spallation Neutron Source (SNS) at Oak Ridge National Laboratory (ORNL) [1]. Although these measurements are vital in obtaining important phonon and crystalline information, it is preferred to have more independent forms of cross section measurements to validate (or evaluate) thermal scattering law (TSL) files. Integral benchmarks and pulsed-neutron die-away measurements serve as a useful tool, but total cross section measurements are ideal to complement the double-differential scattering measurements.

The materials evaluated in this project are all hydrogen rich, meaning they are predominately incoherent scatterers. Therefore, the incoherent Gaussian approximation as implemented in NJOY2016 LEAPR module [2] is sufficient to calculate inelastic scattering in these materials. The NJOY2016 LEAPR module is commonly used for calculation of the incoherent inelastic scattering cross section, $S(\alpha,\beta)$, and the expression can be written as

$$S(\alpha,\beta) = e^{-\alpha\int_{-\infty}^{\infty} P(\beta)e^{-\beta/2}d\beta} \sum_{n=0}^{\infty} \frac{1}{n!}\alpha^n \frac{1}{2\pi} \times \int_{-\infty}^{\infty} e^{i\beta\hat{t}} \left[\int_{-\infty}^{\infty} P(\beta')e^{i\beta'\hat{t}} e^{-\beta'/2} d\beta' \right]^n d\hat{t}, \tag{1}$$

$$P(\beta) = \frac{\rho(\beta)}{2\beta\sinh(\beta/2)} \quad \text{and} \quad W = \frac{\int_{-\infty}^{\infty} P(\beta)e^{-\beta/2}d\beta}{AkT}, \tag{2}$$

where $\rho(\beta)$ is the phonon spectrum and W is the Debye–Waller factor. Coherent elastic scattering is calculated as

$$\sigma^{coh}(E) = \frac{\sigma_c}{E} \sum_{E_i>E} f_i e^{-2WE_i}, \tag{3}$$

and incoherent elastic scattering is calculated as

$$\sigma^{incoh}(E) = \frac{\sigma_b}{2}\left(\frac{1-e^{-4WE}}{2WE}\right). \tag{4}$$

Neutron transmission measurements can be performed at facilities such as the Gaerttner Linear Accelerator (LINAC) Center at Rensselaer Polytechnic Institute (RPI). In a transmission measurement, the measured quantity can be transformed to total cross section, which is the sum of the scattering and capture cross sections. The total scattering cross section is a sum of coherent elastic, coherent inelastic, incoherent elastic, and incoherent inelastic scattering cross sections. In the thermal energy range, the capture cross section is quite well behaved, and most materials have a $1/v$ shape, where v is the neutron velocity. The

simplistic behavior of capture cross section in thermal energy range emphasizes the importance of the scattering cross section and accurate determination of the phonon spectrum.

RPI's work on constructing the new cold moderator system [3, 4, 5] and measurement details [6, 7, 8, 9] has been documented extensively elsewhere and is mentioned only briefly in Section 2. Section 3 outlines ORNL's evaluation work. Section 4 contains some concluding thoughts and ideas for follow-on projects.

2. RPI MEASUREMENTS

The premise of the new cold moderator system is to enhance an already-existing beamline (the RPI Gaerttner LINAC) by placing an apparatus in front of the neutron production target. The system contains a specific material (i.e., cryogenically cooled polyethylene) meant to enhance the thermal neutron flux of the beamline. The benefit of this new enhanced thermal target is that materials in the thermal energy range (e.g., where TSLs are the most important) can be more easily measured.

Four materials were measured at the LINAC and are listed in Table 1: polyethylene (PE), polystyrene (PS), two different samples of poly(methyl methacrylate) (PMMA, denoted here as Plexiglas G and Plexiglas G-UVT for reasons that will be discussed later), and yttrium hydride (YH_x, where the x denotes the different hydrogen concentrations). Each material was also subdivided into two different sample thicknesses (except for the PMMA) to obtain a more complete collection of experimental data over the desired thermal energy range. Summaries of polymer measurements (PE, PS, and PMMA) can be found in a study performed by Fritz et al. [8], whereas a summary of the yttrium hydride measurements can be found in a different study conducted by Fritz et al. [9].

Table 1. Materials Measured at RPI LINAC.

Material	Area (cm^2)	Thickness (mm)	Mass (g)	Areal Density (molecule/barn)
PE	162.269 ± 0.422	1.588	24.0947 ± 0.0002	0.00638 ± 0.00001
	162.512 ± 0.250	2.381	37.0882 ± 0.0007	0.00980 ± 0.00003
PS	160.390 ± 0.335	2.381	37.5789 ± 0.0004	0.01084 ± 0.00002
	160.364 ± 0.425	3.969	61.3445 ± 0.0006	0.01770 ± 0.00005
Plexiglas G-UVT	18.620 ± 0.015	4.674	10.3421 ± 0.0001	0.003340 ± 0.000001
Plexiglas G	18.696 ± 0.015	3.073	6.7688 ± 0.0001	0.002178 ± 0.000001
$YH_{1.85}$	19.502 ± 0.016	2	17.5499 ± 0.0002	0.005864 ± 0.000102
	19.431 ± 0.016	5	43.5656 ± 0.0004	0.014870 ± 0.000003
$YH_{1.68}$	19.268 ± 0.016	2	16.2584 ± 0.0002	0.0056090 ± 0.0000006
	19.205 ± 0.016	5	43.2684 ± 0.0004	0.014970 ± 0.000004

3. ORNL ANALYSIS

3.1 COMPUTATIONAL ATOMISTIC SIMULATION

3.1.1 Polyethylene and Polystyrene

High-density polyethylene $(C_2H_4)_n$ is a hydrocarbon polymer that has a crystalline fraction as high as 80%–90%. Similarly, polystyrene $(C_8H_8)_n$ is also a hydrocarbon polymer that has a significant crystalline fraction, depending on the tacticity of the polymer chains. Because of the similarities between these materials, the methods used to calculate the phonon properties are also very similar. Since the materials have a significant crystalline fraction, they were simulated using the density functional theory (DFT) code CASTEP [10]. The starting configuration for polyethylene was chosen based on work from Barrera et al. [11] and resulted in a unit cell containing 12 atoms (4 carbon, 8 hydrogen), whereas the starting configuration for polystyrene was taken from Natta et al. [12], which expanded into a unit cell containing 48 carbon and 48 hydrogen atoms.

The cells were first relaxed using the Broyden–Fletcher–Goldfarb–Shanno minimization algorithm to identify an energetically stable atomic configuration and unit cell shape. The systems were relaxed until a tolerance of 5×10^{-9} eV/atom for the ground state energy and 5×10^{-4} Å for the geometric displacement of each atom in each material was met. A 750 eV energy cutoff was used in conjunction with a Perdew–Burke–Ernzerhof [13, 14, 15] functional. Internal testing showed that the optimal k-point grid for polyethylene for phonon calculations was $3 \times 5 \times 9$, whereas a k-point grid of $1 \times 1 \times 3$ was sufficient for polystyrene (due to the large size of its unit cell). This relaxed unit cell was then used to calculate phonon properties using CASTEP's built-in density functional perturbation theory (DFPT) method. The advantage to using this method is that the calculations can be performed on the unit cell instead of the (often much larger) supercell. The resulting phonon file was then fed into OCLIMAX [16, 17], which was used to calculate the partial phonon density of states (PDOS). This PDOS was then used to calculate the total cross section using NJOY [2].

3.1.2 Poly(methyl methacrylate)

Although polyethylene and polystyrene could be modeled as a primarily crystalline structure, poly(methyl methacrylate) $(C_5O_2H_8)_n$ (often referred to by its trade name and brand, including Lucite and Plexiglas) is a predominately amorphous polymer material. Therefore, classical molecular dynamics (MD) calculations were carried out using the Large-scale Atomic/Molecular Massively Parallel Simulator (LAMMPS) [18]. The initial structure for MD calculations was obtained using Polymer Builder [19], as implemented in CHARMM-GUI [20]. The structure created by Polymer Builder consisted of 55 chains and 20 monomers of PMMA at each chain.

Polymer Builder automates the creation of relaxed polymer systems and offers diverse modeling methods to construct intricate polymer structures. Furthermore, it can create genuine polymer melt and solution systems by employing both a coarse-grained model and an all-atom replacement. The concept of a coarse-grained model is central in the computational study of complex systems such as polymers, proteins, and more. Essentially, this model works by simplifying a system in which multiple atoms, or even whole molecules, are consolidated and represented as a single entity, often referred to as a "bead" or "particle." This method drastically cuts down on system complexity and computational demands, enabling the study of larger systems or extended time scales that would be impractical with a fully atomistic model.

The relaxed model is then melted using molecular dynamics in LAMMPS using CHARMM force field and quenched to the desired temperature using an NVT ensemble (i.e., the canonical ensemble, where the Number of particles in the system, Volume, and Temperature are kept constant). The system is further equilibrated in an NPT ensemble (i.e., the isothermal-isobaric ensemble, where where the Number of particles in the system, Pressure, and Temperature are kept constant), and the production run is performed using an NVT ensemble. The partial densities of states for each atom were calculated using a velocity auto-correlation function, as implemented in MDANSE [21].

3.1.3 Yttrium Hydride

As part of the Transformational Challenge Reactor (TCR) campaign at ORNL, yttrium hydride was also considered in this project. The exact modeling details are described in Chapman et al.'s study [22] but is outlined briefly in this section. Since the TCR campaign specifically requested a high-temperature evaluation, a new methodology needed to be implemented to account for the anharmonicity known to exist in metal hydrides at higher temperatures. Several methods were considered for simulating both the high-temperature effects, but ultimately the temperature-dependent effective potential (TDEP) method was selected [23, 24, 25]. This process was divided into two steps: (1) calculating the lattice parameters and (2) calculating the forces generated from stochastic sampling of the interatomic force constants (IFCs).

For both steps, the Vienna Ab initio Simulation Package (VASP) [26, 27, 28] was used. Lattice parameters were calculated using the quasi-harmonic approximation and were found to be in good agreement with experimental measurements [29]. With these lattice parameters, force calculations were performed on a $4 \times 4 \times 4$ supercell of a primitive unit cell of YH_2, which contained a total of 64 yttrium and 128 hydrogen atoms. The resulting IFCs were extracted from the VASP runs using TDEP, and these IFCs were then used to stochastically generate new supercells [30]. This process was repeated until the IFCs converged. Once convergence was reached, the partial PDOS was calculated and was then used to calculate the total cross section using NJOY.

3.2 FITTING PROCEDURE

A new fitting procedure was developed to incorporate both the transmission measurements referenced above as well as inelastic neutron scattering (INS) measurements carried out at the Spallation Neutron Source (SNS) at ORNL. The particulars of the fitting procedure and INS measurements will be discussed in a future publication. The PDOS is divided into distinct regions chosen based on the individual features present in the spectrum (e.g., noticeable peaks, changes in the overall shape of the PDOS, relations from PDOS to known material effects). Each region is then varied using Dakota [7] and processed into the INS and transmission spectra using NCrystal [8].

To give a detailed example of this fitting procedure, the PDOS for polyethylene is given in Figure 1 and the resulting fitted PDOS (as well as the original un-fitted PDOS) are shown in Figure 2. In this example, the PDOS was subdivided into seven unique regions, predominately corresponding to sharp features in the PDOS. The resulting change in PDOS is most noticeable in the varying magnitudes of the peaks in the 0.15–0.20 eV region.

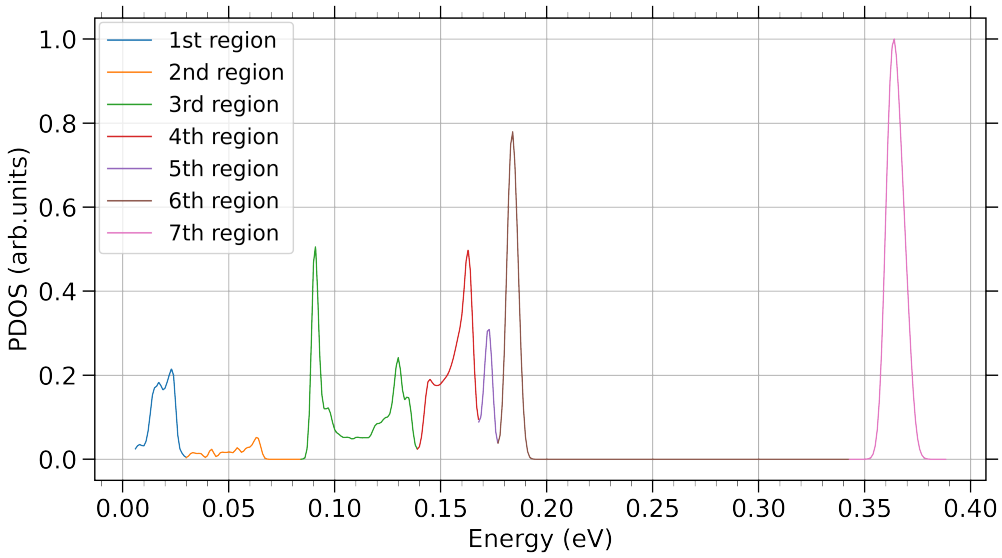

Figure 1. Polyethylene PDOS subdivided into regions for fitting.

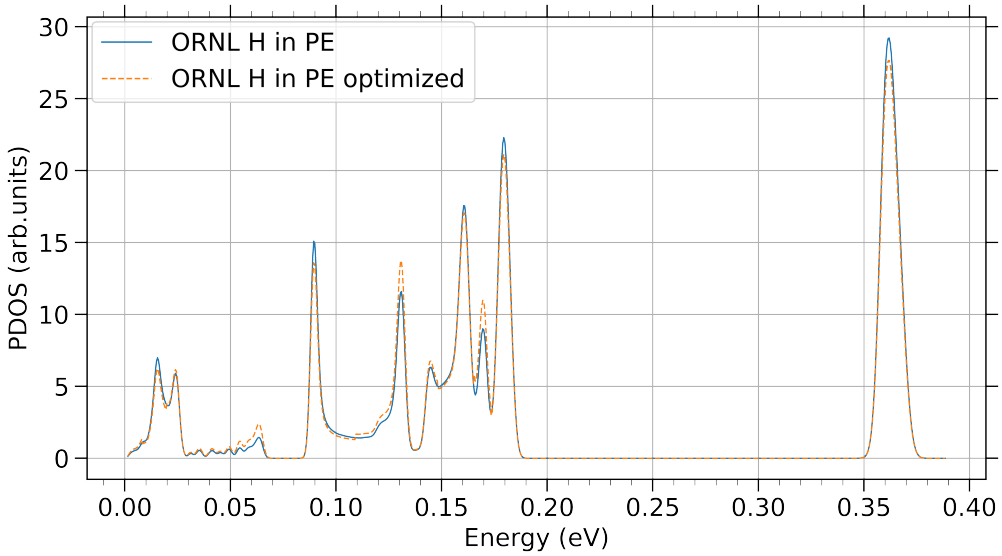

Figure 2. Polyethylene PDOS comparison before and after fitting procedure.

3.3 COMPARISON TO EXPERIMENTS

3.3.1 Polyethylene

Using the methodology described above, the newly fitted PE cross section (labeled as ORNL) as well as the ENDF/B-VIII.0 cross section are shown with the RPI measured data in Figure 3. Additionally, a ratio of the calculated-to-experimental (C/E) results plot of the ORNL and ENDF/B-VIII.0 files against the experimental uncertainties of the RPI measurements are shown.

Although both files show moderate agreement with the experimental data, the C/E plot shows the impact of

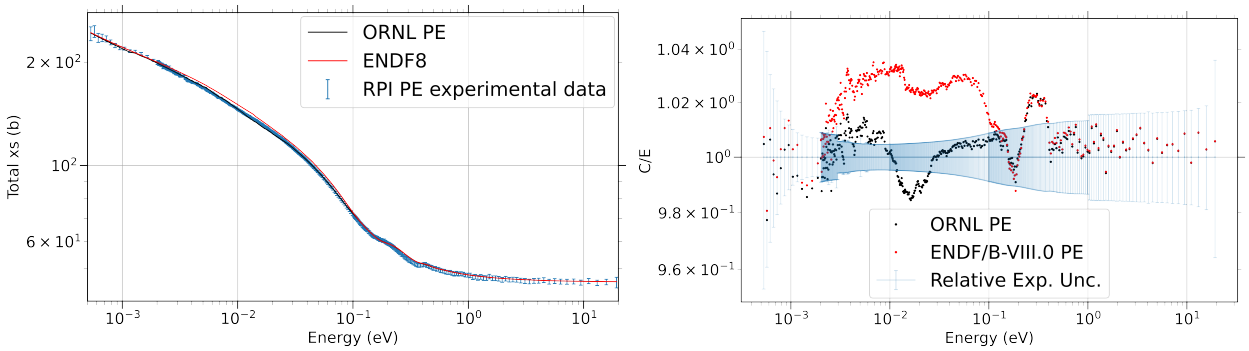

Figure 3. Polyethylene Total XS comparison with ORNL and ENDF/B-VIII.0 files and C/E plot.

the fitting procedure. Specifically, the region between 3×10^{-3} eV and 1×10^{-1} eV shows the most noticeable difference between the datasets. Even with the ORNL files underestimating the cross section between 1×10^{-2} eV and 2.5×10^{-2} eV, the overall agreement is better with the ORNL dataset. It is also worth noting that the ORNL files include coherent elastic contributions in the C-CH2 TSL file. The inclusion of these contributions is partially because polyethylene is a crystalline material and should, therefore, exhibit crystalline features (such as Bragg edges in coherent elastic scattering), but also because the total cross section measurements indicate a very minor set of Bragg edges.

3.3.2 Polystyrene

The fitted PS cross section, along with the RPI measured data, are shown in Figure 4. Despite there being no previous evaluation for polystyrene, the agreement with the total cross section is very good. The only noticeable deviation in the C/E plot occurs between 2 meV and 10 meV, and even that deviation is quite small.

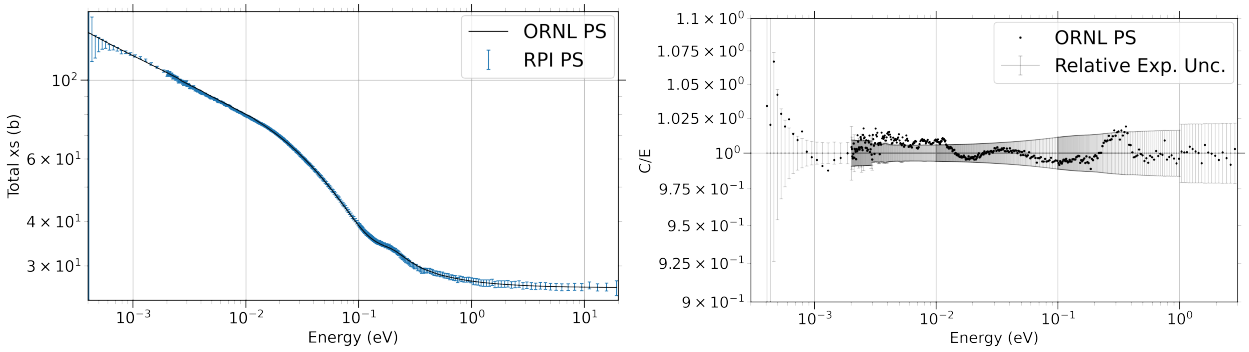

Figure 4. Polystyrene total cross section comparison with ORNL file and C/E plot.

The primary reason for performing a polystyrene evaluation was calculations of criticality benchmarks that contained polystyrene were using the polyethylene TSL as a surrogate. It was unclear whether using the surrogate was a suitable substitute. The critical benchmarks have since been shown to be suboptimal for comparing the two [31]. With that in mind, a C/E plot comparing the ORNL polyethylene library and ORNL polystyrene library with the polystyrene measurement is shown in Figure 5. Although the cross sections show a noticeable difference from one another, the lack of differences in integral benchmarks [31]

is in line with recent studies suggesting that integral critical benchmarks might not be best suited for determining an optimal TSL cross section when the cross sections are close to one another [32].

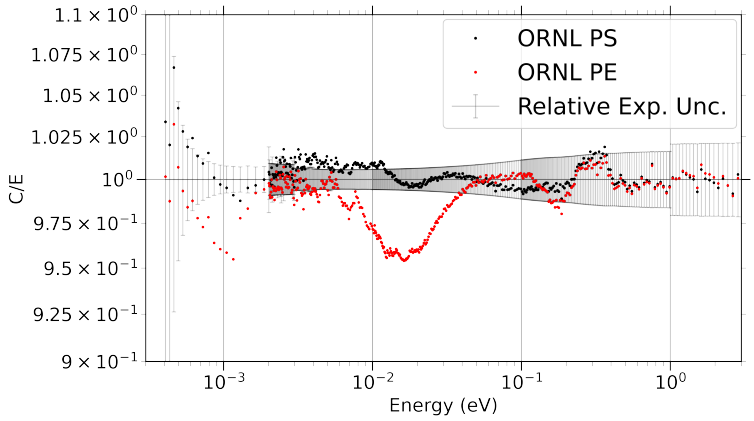

Figure 5. Comparison of polyethylene and polystyrene files against polystyrene total cross section.

3.3.3 Poly(methyl methacrylate)

For the PMMA measurements, the comparison of the ENDF/B-VIII.0 library, ORNL evaluation, and updated library from North Carolina State University (NCSU) with the total cross section measurements is shown in Figure 6. The C/E plot shown on the right corresponds with the measurements of Plexiglass G, with which all three libraries are in better agreement compared to Plexiglass G-UVT. The decision to fit the Plexiglass G sample instead of the Plexiglass G-UVT sample was made because Plexiglass G is a more widely used commercial form of the material and is thus more likely to be used in a wide range of applications [8], despite Plexiglass G-UVT being the more chemically pure sample (i.e., fewer additives or impurities), and therefore closer to 'true' PMMA.

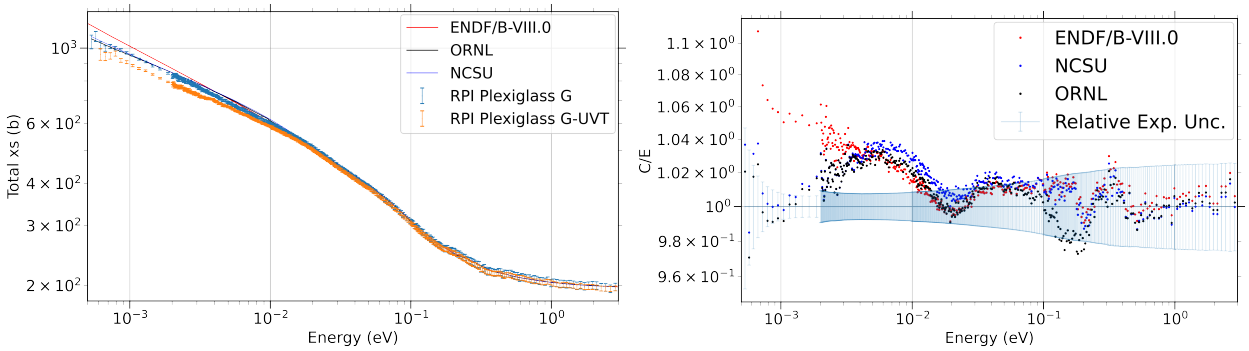

Figure 6. Plexiglas Total XS comparison with ORNL, ENDF/B-VIII.0, and NCSU files and C/E plot.

Clearly, the ENDF/B-VIII.0 library overpredicts the cross section at energies below 2 meV. Comparing the NCSU and ORNL libraries is more easily seen in the C/E plot, where the ORNL library shows better agreement in the 5 meV–100 meV range. Although the ORNL library dips significantly between 100 meV and 200 meV (compared to the ENDF/B-VIII.0 and NCSU libraries), the values are still largely within the experimental uncertainty of the measured data.

3.3.4 Yttrium Hydride

Due to the needs of the TCR program, more focus was placed on correctly modeling high-temperature differential scattering. As such, the optimization and fitting techniques described in Section 3.3.3 has not yet been implemented for the YH_x files. Plots showing the comparison of the two samples with the ENDF/B-VIII.0 and ORNL libraries are shown in Figure 7.

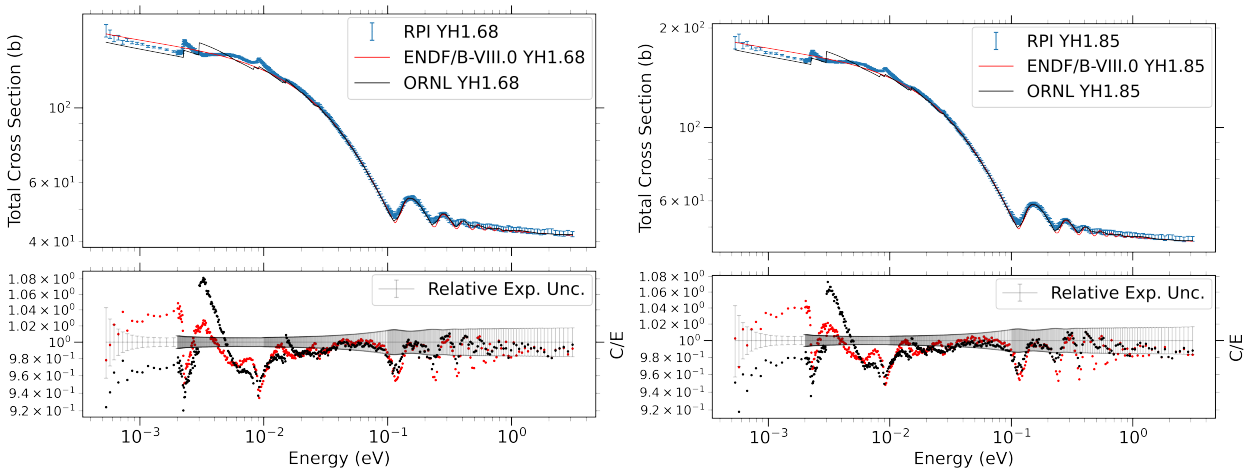

Figure 7. Yttrium hydride total cross section comparison with ORNL and ENDF/B-VIII.0 and C/E plot.

Although the disagreement between the experimental data and the evaluations is apparent, there are a few areas of noticeable improvement. The ORNL evaluation includes coherent elastic effects in the evaluation, as Bragg edges can be clearly seen between 2 meV and 10 meV. Additionally, there is significantly better agreement in the multi-phonon scattering region about 100 meV.

4. CONCLUSIONS

Total cross section measurements from a recently installed cold moderator system at the RPI Gaerttner LINAC were used to evaluate materials of interest for the Nuclear Criticality Safety Program. Specifically, polyethylene, polystyrene, and poly(methyl methacrylate) were evaluated by fitting theoretical models for these materials to the RPI total cross sections and to SNS-measured INS data. These newly fitted data have been shown to be in favorable agreement with the cross sections to which they were fitted (which is expected), and further analysis on their agreement with available differential scattering data, as well as their impact to integral criticality benchmarks, will be detailed in future publications. The corresponding ENDF files for polyethylene, polystyrene, and poly(methyl methacrylate) have been submitted to the National Nuclear Data Center for consideration in the upcoming ENDF/B-VIII.1 library.

The fitting procedure has not yet been carried out with the yttrium hydride measurements because high-temperature simulation modeling still requires refinement. The yttrium hydride analysis is ongoing, with the plan of completing the fit and high-temperature analysis by the end of 2023. Additionally, because of the nature of the fitting procedure, it is theoretically possible to obtain covariance data for these materials. This was not done here, as there is no agreed-upon method for processing, storing, and using TSL covariance data; however, such data could be used in future analyses once these methods are developed.

This work was supported by the Nuclear Criticality Safety Program, funded and managed by the National Nuclear Security Administration for the Department of Energy.

5. REFERENCES

[1] Chris W. Chapman, Xunxiang Hu, Jesse Brown, Goran Arbanas, Kemal Ramić, Alexander I. Kolesnikov, Matt Stone, Douglas L. Abernathy, Yongqiang Cheng, Luke Daemen, Anibal Ramirez Cuesta, Li (Emily) Liu, and Yaron Danon. Thermal Neutron Scattering Measurements and Evaluations at ORNL. Nuclear Criticality Safety Program (NCSP) Technical Program Review 2021, 23-25 February 2021, Oak Ridge, TN, https://ncsp.llnl.gov/sites/ncsp/files/2021-05/56_TNS_measurements_at_ORNL_2021_TPR_final.pdf.

[2] R.E. MacFarlane and A.C. Kahler. Methods for Processing ENDF/B-VII with NJOY. *Nuclear Data Sheets*, 111(12):2739–2890, 2010. Nuclear Reaction Data.

[3] Dominik Fritz. *Design of a Cold Moderator for Total Cross Section Measurements of Moderator Materials at Sub-Thermal Energies*. PhD thesis, 2022. https://www.proquest.com/dissertations-theses/design-cold-moderator-total-cross-section/docview/2769190497/se-2.

[4] Dominik A. Fritz and Yaron Danon. A Cold Moderator For Sub-Thermal Neutron Flux Enhancement at the RPI-LINAC. *Transactions of the American Nuclear Society*, 123(1), 11 2020.

[5] D. Fritz, Y. Danon, and E. Liu. Enhancement of sub-thermal neutron flux through cold polyethylene. *Journal of Neutron Research*, 23(2-3), 9 2021.

[6] Yaron Danon, Dominik Fritz, Benjamin Wang, Katelyn Cook, Sukhjinder Singh, Adam Ney, Peter Brain, Ezekiel Blain, Michael Rapp, Adam Daskalakis, Devin Barry, Timothy Trumbull, Chris Chapman, and Goran Arbanas. Experimental validation of thermal scattering evaluations. *EPJ Web of Conf.*, 284:17001, 2023.

[7] Dominik Fritz, Yaron Danon, Michael Rapp, Timothy Trumbull, Michael Zerkle, Jesse Holmes, Chris Chapman, Goran Arbanas, Jesse Brown, Kemal Ramic, Xunxiang Hu, Adam Ney, Peter Brain, Sukhjinder Singh, Katelyn Cook, and Benjamin Wang. Thermal Cross Section Measurements At The RPI LINAC. *EPJ Web of Conf.*, 284:01020, 2023.

[8] D. Fritz, Y. Danon, K. Ramic, C. W. Chapman, J. M. Brown, G. Arbanas, M. Rapp, T. H. Trumbull, M. Zerkle, J. Holmes, P. Brain, A. Ney, S. Singh, K. Cook, and B. Wang. Total thermal neutron cross section measurements of hydrogen dense polymers from 0.0005 - 20 eV. *Annals of Nuclear Energy (Oxford)*, 183, 12 2022.

[9] Dominik A. Fritz, Yaron Danon, Michael J. Rapp, Timothy H. Trumbull, Michael L. Zerkle, Jesse C. Holmes, Chris W. Chapman, Goran Arbanas, Jesse M. Brown, Kemal Ramic, Xunxiang Hu, Sukhjinder Singh, Adam Ney, Peter Brain, Katelyn Cook, and Benjamin Wang. Total thermal neutron cross section measurements of yttrium hydride from 0.0005 - 3 eV. *Annals of Nuclear Energy (Oxford)*, 181(3), 10 2022.

[10] S. J. Clark, M. D. Segall, C. J. Pickard, P. J. Hasnip, M. J. Probert, K. Refson, and M.C. Payne. First principles methods using CASTEP. *Z. Kristall.*, 220:567–570, 2005.

[11] Gustavo D. Barrera, Stewart F. Parker, Anibal J. Ramirez-Cuesta, and Philip C. H. Mitchell. The Vibrational Spectrum and Ultimate Modulus of Polyethylene. *Macromolecules*, 39(7):2683–2690, 2006.

[12] G Natta, P Corradini, and IW Bassi. Crystal structure of isotactic polystyrene. *Nuovo Cimento*, 15(S1):68–82, 1960.

[13] G. Kresse and D. Joubert. From ultrasoft pseudopotentials to the projector augmented-wave method. *Phys. Rev. B*, 59:1758–1775, Jan 1999.

[14] John P. Perdew, Kieron Burke, and Matthias Ernzerhof. Generalized Gradient Approximation Made Simple. *Phys. Rev. Lett.*, 77:3865–3868, Oct 1996.

[15] John P. Perdew, Kieron Burke, and Matthias Ernzerhof. Generalized Gradient Approximation Made Simple [Phys. Rev. Lett. 77, 3865 (1996)]. *Phys. Rev. Lett.*, 78:1396–1396, Feb 1997.

[16] Y. Q. Cheng, L. L. Daemen, A. I. Kolesnikov, and A. J. Ramirez-Cuesta. Simulation of Inelastic Neutron Scattering Spectra Using OCLIMAX. *Journal of Chemical Theory and Computation*, 15(3):1974–1982, 2019. PMID: 30735379.

[17] Y. Q. Cheng and A. J. Ramirez-Cuesta. Calculation of the Thermal Neutron Scattering Cross-Section of Solids Using OCLIMAX. *Journal of Chemical Theory and Computation*, 16(8):5212–5217, 2020. PMID: 32700910.

[18] A. P. Thompson et al. LAMMPS- a flexible simulation tool for particle-based materials modeling at the atomic, meso and continuum scales. *Computational Physics Communications*, 271, 2022.

[19] Yeol Kyo Choi, Sang-Jun Park, Soohyung Park, Seonghoon Kim, Nathan R. Kern, Jumin Lee, and Wonpil Im. CHARMM-GUI Polymer Builder for Modeling and Simulation of Synthetic Polymers. *Journal of Chemical Theory and Computation*, 17(4):2431–2443, 2021. PMID: 33797913.

[20] Sunhwan Jo, Taehoon Kim, Vidyashankara G. Iyer, and Wonpil Im. Charmm-gui: A web-based graphical user interface for charmm. *Journal of Computational Chemistry*, 29(11):1859–1865, 2008.

[21] G. Goret, B. Aoun, and E. Pellegrini. MDANSE: An Interactive Analysis Environment for Molecular Dynamics Simulations. *Journal of Chemical Information and Modeling*, 57(1):1–5, 2017. PMID: 28026944.

[22] Chris W. Chapman, Kemal Ramić, Xunxiang Hu, Jesse M. Brown, Goran Arbanas, Alexander I. Kolesnikov, Douglas L. Abernathy, Luke Daemen, Anibal (Timmy) J. Ramirez-Cuesta, Yongqiang Cheng, Matthew B. Stone, Li (Emily) Liu, and Yaron Danon. Thermal neutron scattering measurements and modeling of yttrium-hydrides for high temperature moderator applications. *Annals of Nuclear Energy*, 157:108224, 2021.

[23] Olle Hellman and I. A. Abrikosov. Temperature-dependent effective third-order interatomic force constants from first principles. *Phys. Rev. B*, 88:144301, Oct 2013.

[24] O. Hellman, I. A. Abrikosov, and S. I. Simak. Lattice dynamics of anharmonic solids from first principles. *Phys. Rev. B*, 84:180301, Nov 2011.

[25] Olle Hellman, Peter Steneteg, I. A. Abrikosov, and S. I. Simak. Temperature dependent effective potential method for accurate free energy calculations of solids. *Phys. Rev. B*, 87:104111, Mar 2013.

[26] G. Kresse and J. Furthmüller. Efficiency of ab-initio total energy calculations for metals and semiconductors using a plane-wave basis set. *Computational Materials Science*, 6(1):15–50, 1996.

[27] G. Kresse and J. Furthmüller. Efficient iterative schemes for ab initio total-energy calculations using a plane-wave basis set. *Phys. Rev. B*, 54:11169–11186, Oct 1996.

[28] G. Kresse and J. Hafner. Ab initio molecular dynamics for liquid metals. *Phys. Rev. B*, 47:558–561, Jan 1993.

[29] J. N. Daou and P. Vajda. Hydrogen ordering and metal-semiconductor transitions in the system yh_{2+x}. *Phys. Rev. B*, 45:10907–10913, May 1992.

[30] Nina Shulumba, Olle Hellman, and Austin J. Minnich. Intrinsic localized mode and low thermal conductivity of PbSe. *Phys. Rev. B*, 95:014302, Jan 2017.

[31] C. W. Chapman, K Ramic, G. Arbanas, J. Brown, A. Kolesnikov, Matthew Stone, L. Daemen, Y. Cheng, A. Cuesta, Y. Danon, and D. Fritz. Applying Methodology for Evaluating and Validating TSLs to Materials of Interest to NCSP. Nuclear Criticality Safety Program (NCSP) Technical Program Review 2023, 21-23 February 2023, Albuquerque, NM, https://ncsp.llnl.gov/sites/ncsp/files/2023-03/58_tpr2023_chapman_tsl_final.pdf.

[32] K. Ramic, C. W. Chapman, G. Arbanas, J. Brown, B.J. Marshall, L. Daemen, D. Abernathy, A. Kolesnikov, Y. Cheng, A. Cuesta, D. Siefman, Y. Danon, and D. Fritz. On integral benchmarks for resolving TSL conflicts for ENDF/B-VIII.1 release. https://indico.bnl.gov/event/18702/contributions/75651/attachments/47377/80341/mini_CSWEG_2023_on_integral_benchmarks.pdf, 2023.